ADVANCED MATERIALS TECHNOLOGIES
www.advmattechnol.de

Screen-Printed, Low-Cost, and Patterned Flexible Heater Based on Ag Fractal Dendrites for Human Wearable Application

*Pan Zeng, Bin Tian, Qingyong Tian, Weijing Yao, Mengxiao Li, Huanjun Wang, Yu Feng, Li Liu, and Wei Wu**

Achieving all-printed, low-cost, and large area electronic devices poses challenging requirements in employing printing technologies and conductive materials for flexible and wearable heaters. In this work, fully printed, scalable, and patterned flexible heaters based on Ag fractal dendrites (FDs) are fabricated through straightforward screen printing technology. The Ag FDs possess low sheet resistance with ≈0.83 Ω sq^{-1} when sintered at low temperature of 60 °C. The Ag FDs are directly printed on thin polyethylene terephthalate substrate to manufacture flexible heaters, exhibiting excellent heating performance with the saturation temperature up to ≈135 °C and rapid response time within 35 s under 4 V DC voltage. In addition, the Ag FDs heaters present lower power consumption (≈209.67 °C cm^2 W^{-1}), which is significantly better than traditional indium tin oxides (ITO) heaters (≈88 °C cm^2 W^{-1}). The sheet resistance of the devices remains stable after 2000 bending cycles with a radius of 10 mm, indicating that the outstanding mechanize stability of the heaters. Moreover, a large area (12 cm × 5 cm) heater with designable pattern is developed and attached to human body, indicating a bright future in next-generation fully printed and wearable heating electronics application.

1. Introduction

Printed electronics technology attracts remarkable attention during the past few decades,[1] and the market size is predicted with a prosperous development to $300 million in the next 20 years.[2] A lot of electronic devices have been made by printed electronic techniques, such as radio frequency identification tags,[3,4] thin-film transistors (TFTs),[5–7] light-emitting diodes (LEDs),[8,9] sensors,[10,11] supercapacitors,[1,12–14] and organic light-emitting diodes.[15,16] Recently, printed flexible resistance heaters have drawn noteworthy interests because of their widespread applications in medical and advanced wearable thermotherapy devices.[17,18] For example, human joints are often injured because of obesity, occupational overuse, or aging. Joint injured often leads to many symptoms, such as pain, swelling, and muscle weakness, and thermotherapy was widely used to improve these symptoms.[19,20] Thermotherapy is one of the classic orthopedic treatments, which have been usually used to treat rheumatic arthritis, cervical spondylosis, and traumatic injuries.[21]

Currently, various printed electronic techniques have been applied to manufacture flexible resistance heaters, such as bar coating.[22,23] spin coating,[18,24] spray printing,[25–27] and transfer printing.[28,29] However, these techniques are either expensive or unsuitable for large-scale fabrication, resulting in high costs finally. To overcome these problems, screen printing is an ideal candidate for manufacturing flexible electronics, which is low cost, large-scale, and versatile pattern designs.[30] In addition, the fabricating technique is simplicity and less waste.[31] For example, we used the fully screen printing method to fabricate the high performance flexible supercapacitors[12,32] in recently, and other research group also fabricated the all-printed TFT[33] and solar cells[34] by employing this technology, which demonstrate that the great progresses are achieved in the flied of printed flexible electronics. Consequently, screen printing technology is perfect options for flexible heater, which can realize different areas, versatile pattern and can be printed on various substrate, for instance, textile, polyethylene terephthalate (PET), and polyvinyl alcohol (PVA).

Up to now, various conductive materials have been developed by researchers for realizing the optimal performance of the printed flexible resistance heaters. Traditional conductive materials, such as metallic nanowires (NWs),[26,35,36] carbon nanotube

P. Zeng, B. Tian, Q. Y. Tian, W. J. Yao, M. X. Li, H. J. Wang, Y. Feng, L. Li, Prof. W. Wu
Laboratory of Printable Functional Nanomaterials and Printed Electronics
School of Printing and Packaging
Wuhan University
Wuhan 430072, P. R. China
E-mail: weiwu@whu.edu.cn
Prof. W. Wu
National and Local Joint Engineering Research Center of Advanced Packaging Materials Developing Technology
Hunan University of Technology
Zhuzhou 412007, P. R. China
Prof. W. Wu
Shenzhen Research Institute of Wuhan University
Shenzhen 518057, P. R. China
The ORCID identification number(s) for the author(s) of this article can be found under https://doi.org/10.1002/admt.201800453.

DOI: 10.1002/admt.201800453

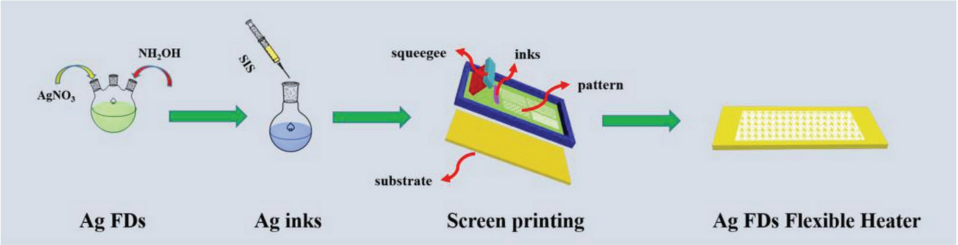

Scheme 1. Schematic illustration of the synthesis of Ag FDs and fabrication process of fully printed flexible heaters.

(CNT),[37–40]graphene,[41–43] conductive polymers,[44,45] and other hybrid materials,[46–51] are widely used in flexible resistance heaters. However, conventional CNT, graphene, and conductive polymers poly(3,4-ethylenedioxythiophene) polystyrene sulfonate (PEDOT: PSS) feature the disadvantage of high resistance, which means high input voltage is required to reach the same heating saturation temperature. In addition, the large-scale preparation processes of CNT and graphene are complicated, which raise the cost and limit scalability. Comparatively, the metallic NWs (e.g., Ag NWs) not only possess outstanding conductivity but also their preparation process is uncomplicated, feasible and no harsh experiment conditions are required. However, the excellent performance is obtained through high temperature sintering (>200 °C), which is misconceived for practical utilization. Therefore, a low sintering temperature is essential for flexible heaters that employ thermosensitive substrate, for example, polyethylene naphthalate, PVA, polycarbonate, and cloth.

As a completely alternative, Ag FDs are synthesized without any capping agents, which can be used to manufacture high performance flexible heaters. And the Ag FDs possess the classical 3D radial configuration and a lot of nanosized surface tips, instead of other nanoparticles (such as nanowires and nanoflakes) with an anisotropic configuration and few surface nanosized structure.[52] Take advantage of the above merits, the Ag FDs-based flexible heater is fabricated by screen printing, which exhibited excellent low-temperature sintering performance and form a good conductive network at low sintering temperature (<80 °C). Therefore, the Ag FDs show great promise to improve high-performance flexible heaters.

In this work, the Ag FDs are synthesized through one-step redox reaction of $AgNO_3$, which is easily to obtain mass products. The whole synthesis process operates at room temperature and no harsh experimental conditions are required. The inks were formulated by mixing polystyrene-*block*-polyisoprene-*block*-polystyrene (SIS) with Ag FDs at the content of ≈30 wt% and then used for screen printing to fabricate flexible resistance heaters. The effect of different line width, printing area on heating performance, and the mechanize stability of the flexible resistance heaters are studied. The large area heater is affixed to human wrist under a light-weight portable energy (≈5 V) and the heat dissipation was efficiently transferred to skin.

2. Results and Discussion

The designed way for the manufacture of the low-cost, high-performance, and versatile patterns printable flexible heaters is presented in **Scheme 1**. First, the Ag FDs were synthesized via one-step redox reaction at room temperature. Subsequently, the inks were prepared through simple mixing the Ag FDs with SIS solution in a certain proportion. Finally, the flexible heaters with versatile patterns were fabricated through screen printing technology, and then sintered at 60 °C for 60 min.

Figure 1a shows the scanning electron microscope (SEM) image of the Ag FDs. The Ag FDs have two levels of branches, the main branches with an average size of 3 µm and have abundant nanosized minor branches. As presented in Figure 1b, high-resolution SEM image confirms that the size of the minor branches is around 300 nm. That is consistent with the result observed from transmission electron microscope (TEM) image in Figure 1c. Figure 1d presents X-ray diffraction (XRD) patterns with the peaks at 38.1°, 44.3°, 64.4°, 77.5°, and 81.5°, which are characteristic of the Ag (Joint Committee on Powder Diffraction Standards (JCPDS) 04-0783). No other diffraction peaks are observed, confirming the high purity of the Ag FDs. Additionally, the lattice fringes of the Ag FDs display interplanar spacings of 0.236 and 0.204 nm in the particle (Figure S1, Supporting Information), which match well with those of the (111) and the (200) planes of the Ag, respectively. Figure S2 in the Supporting Information shows that the SEM images of the Ag FDs layer printed on PET with a thickness of 150 µm annealed at 60 °C for 1 h. As shown in Figure S2a,b in the Supporting Information, the top view SEM images of the Ag FDs/PET film show a uniform distribution of the Ag FDs, indicating that the Ag FDs are connected well with each other after sintering, forming a good conductive path. Figure S2c in the Supporting Information presents the cross-section SEM image of the Ag FDs/PET, the height of the Ag FDs layer is only 13.5 µm. The low sheet resistance (≈0.83 Ω sq^{-1}) is attributed to the unique nanosized tips of Ag FDs, which can be fused and further formed a good 3D conductive network via simple sintering process at 60 °C. As far as we know, this is the first report of using Ag FDs to fabricate flexible heaters.

The structure of the Ag FDs flexible heater is schematic illustrated in **Figure 2**a. The electric current flows through the heater when a DC voltage is applied to the electrodes at two sides of the heaters. And power dissipated drives by resistive joule heating in the Ag FDs network is given by[53]

$$P = \frac{U^2}{R} = I^2 R \tag{1}$$

where P is the power, U is the DC voltage, I is the current, and R is the resistance of the Ag FDs flexible heater. The heat transfer of the Ag FDs flexible heater mainly includes three aspects, conduction, convection, and radiation.[54] Among

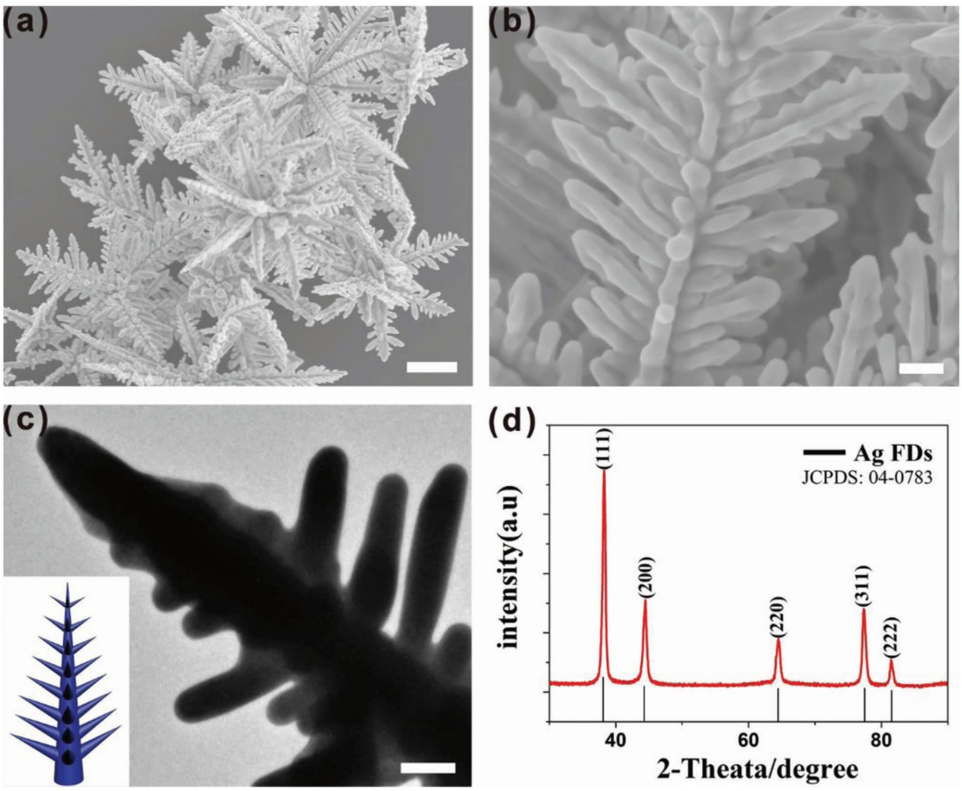

Figure 1. a) Low-magnification SEM image of the Ag FDs (scale bar, 1 μm). b) High-magnification SEM image of the Ag FDs (scale bar, 200 nm). c) TEM image of the Ag FDs and the inset is the detailed morphology of virtual branch of the Ag FDs (scale bar, 200 nm). d) XRD pattern of the Ag FDs.

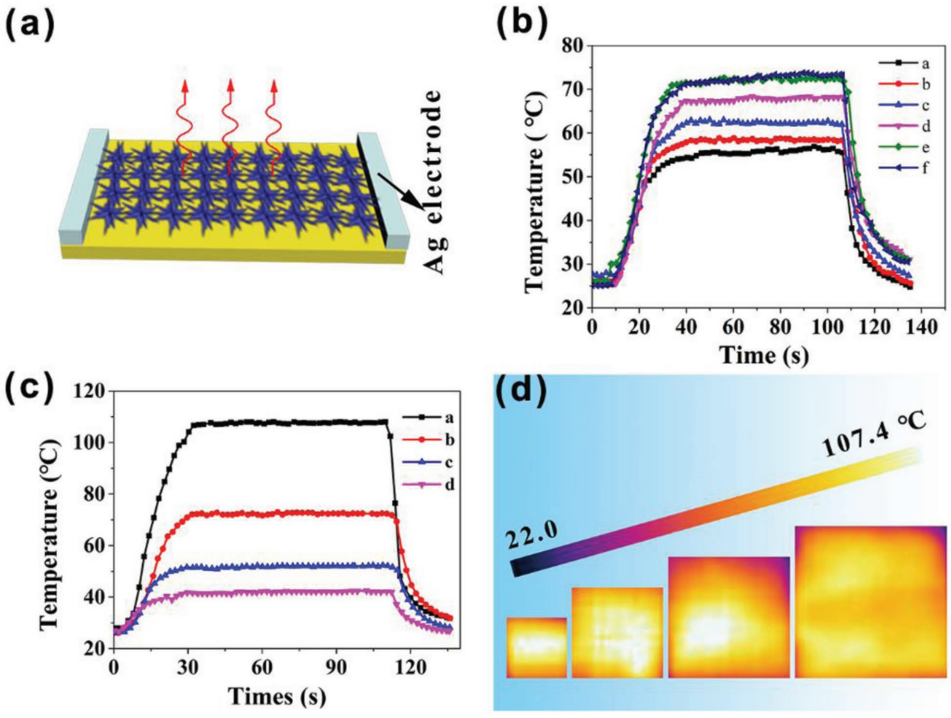

Figure 2. a) Schematic illustration of the flexible heaters with Ag FDs networks. b) The heating performance of the Ag FDs flexible heater with different line width under 2 V, a, b, c, d, e, and f correspond to the 0.2, 0.4, 0.6, 0.8, 1.0, and 1.2 mm of line width, respectively. c) The heating performance of the Ag FDs flexible heaters with different heating area (line width, 1 mm) under the same voltage. d) Thermal photographs of the different heating area under 2 V correspond to 2 cm × 2 cm, 3 cm × 3 cm, 4 cm × 4 cm, and 5 cm × 5 cm, respectively.

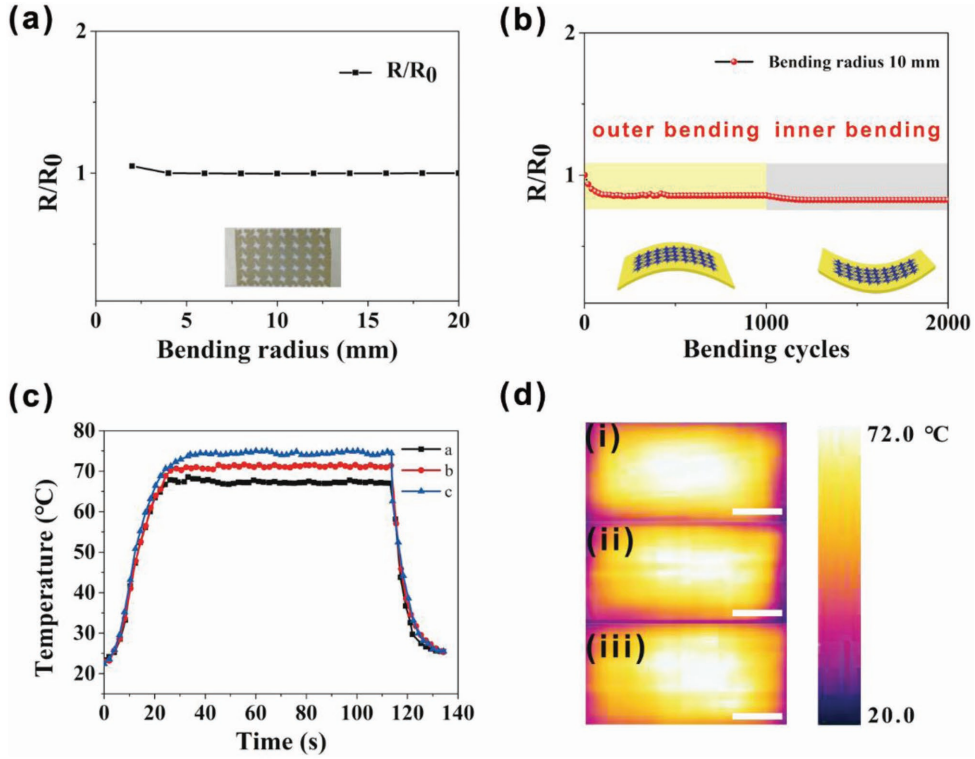

Figure 3. a) Sheet resistance of the Ag FDs flexible heater as a function of bending radius. b) Sheet resistance of the Ag FDs flexible heater as a function of bending cycle. c) Time–temperature profile lines of the Ag FDs flexible heater, a, b, and c correspond to before bending cycles, 1000 cycles of outer bending and after 1000 cycles of inner bending, respectively. d) Thermal photographs of the Ag FDs flexible heater of before bending cycles, after 1000 outer bending cycles and continue for 1000 inner bending cycles (scale bar, 1 cm) under 2 V DC voltage.

them, conduction is the principal way of the heat dissipation, which occurs on between the Ag FDs layer and the substrate, leading to the increment of temperature. Radiation and convection are major factors that bring about heat loss, which happens in between the surrounding air and the Ag FDs layer.

Figure 2b demonstrates the effect of line widths on the heating performance of the heaters. It is shown that the saturation temperature of the devices increases gradually and then becomes stable as the printing line width enlargers. The saturation temperatures are ≈54, 57, 62, 68, 72, and 73 °C, corresponding to the line width of 0.2, 0.4, 0.6, 0.8, 1.0, and 1.2 mm, and the response time of these heaters are about within 35 s. The detailed thermal photographs and digital photographs of the heaters, as shown in Figure S3 in the Supporting Information, are indicating that the heater with line width of 1.0 and 1.2 mm has good heating properties. However, the cost of fabricating flexible heaters needs to be taken into account. Wide printing line requires large amount of Ag FDs, which means higher cost in manufacturing the heaters. Thus, line width of 1 mm is optimum to select because of the combination of cost-effective and good heating performance in an efficient approach.

To investigate the effect of heating areas on the flexible heaters, the heating performance of the heaters with different heating areas are tested. The saturation temperatures decrease from 107 to 41 °C, as the heating area changes from 2 cm × 2 cm to 5 cm × 5 cm, as shown in Figure 2c. The reason is that the radiation and convection volume increase caused by the enlarger of contact area between the Ag FDs layer and the surrounding air. Figure 2d presents the detailed thermal photographs, demonstrating that the heating is uniform because of the excellent conductivity and thermal stability performance of the Ag FDs. Figure S4 in the Supporting Information shows the digital photographs of the heater with different heating area.

Outstanding mechanical flexibility performance is important for wearable electronics. As shown in **Figure 3**, we study the relative sheet resistance change of the Ag FDs flexible heater under the effect of bending. Figure 3a presents the sheet resistance change is negligible when the bending radius is reduced to 2 mm. The devices maintain outstanding conductivity under deformation because of the addition of the SIS rubber in inks formulation. Moreover, Figure 3b shows that the Ag FDs heater is tested repeatedly for 2000 cycles with a bending radius of 10 mm, including the outer bending and inner bending are 1000 times, respectively. During the outer bending cycles, the resistance of the Ag FDs flexible heater decreases to around 85.52% of the initial value and then keeps stable. The decrease of the sheet resistance of the heater after bending cycles attributed to compression of the Ag FDs layer caused by bending. The inner bending process is similar to the outer bending process, but the resistance is subsequently decreased to 82.48% of the initial value. Supposedly the cyclic compressive or tensile stress can promote the compression of the Ag FDs layer and the compression of Ag FDs layer causes

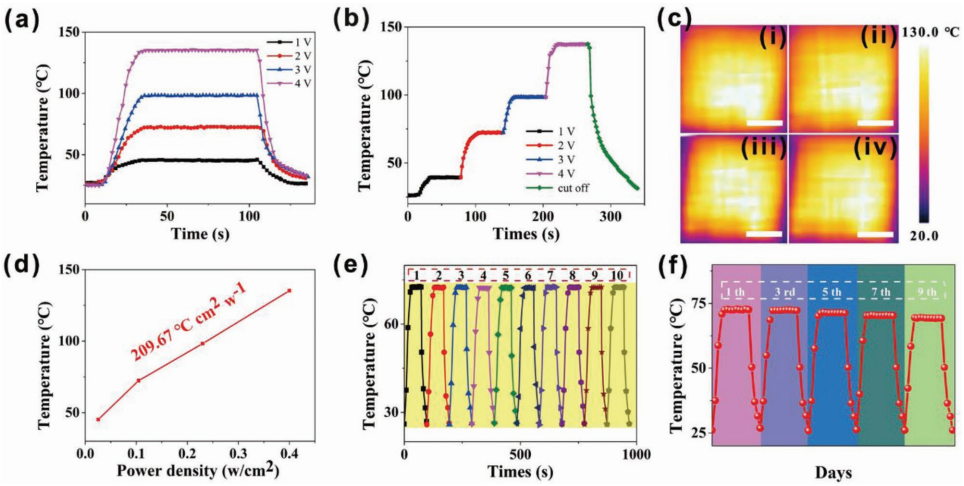

Figure 4. (a) and (b) show the time–temperature profile lines of the Ag FDs flexible heater (line width 1 mm) operated at different voltage. c) Thermal photograph of the Ag FDs flexible heater (line width 1 mm) under different biases: i) 1 V, ii) 2 V, iii) 3 V, and iv) 4 V (scale bars, 1 cm). d) Temperature versus the input power density for the Ag FDs flexible heater. e) Heating cycles of the Ag FDs flexible heater. f) Temperature response of the Ag FDs flexible heater over nine heating cycles.

originally unconnected Ag FDs touched and formed good conductive networks.[55–57] Identical conclusion is obtained in studies of the heating performance where the same DC voltage is applied to the Ag FDs flexible heater before and after bending, respectively. Figure 3c shows the time–temperature profile lines of the Ag FDs flexible heater before and after bending, the saturation temperature is rising, around 69, 71, and 73 °C, respectively. Figure 3d presents the corresponding thermal photographs of the heater before and after bending cycles. Moreover, we use the Ag FDs-based inks to print a pattern on paper, which can be used as a conductor to light an LED, even if the Ag FDs/paper is folded into an origami crane (Figure S5a, Supporting Information).

The saturation temperature of the heaters can be defined by[58]

$$T_{\mathrm{Sat}} = \left(\frac{V^2}{R} - Q_{\mathrm{d}}\right) / Cm + T_0 \tag{2}$$

where T_0 is the room temperature, Q_{d} is the total heat dissipated, C is the heat capacity, and m is the mass.[58] The response time of the heaters can be defined as the time required to rise to the saturation temperature. **Figure 4**a,b shows the time-dependent temperatures profile lines of the heaters with same sheet resistance under different voltages. The temperature of the heaters rapidly increases after the voltage is applied and reaches the saturation temperature within 35 s. When the power is cut off, the temperature decreases quickly. The saturation temperatures of the devices are about 45, 72, 98, and 135 °C under 1, 2, 3, and 4 V DC voltage, respectively. Furthermore, we compared with other previous heaters, such as Ag NWs-, CNT-, and graphene-based heaters (Figure S5b, Supporting Information). The heating performance of the Ag FDs flexible heaters are better than other types of heaters. Figure 4c shows the detailed thermal photographs of the heater under different voltages. Moreover, Figure 4d demonstrates the temperature as a function of the input power density for the Ag FDs flexible heater. The temperature and power density are approximately linear and the slope is very steep (≈209.67 °C cm^2 W^{-1}), indicating the low power consumption of the devices, which is better than heaters based on ITO heaters.[47] The current–voltage and voltage–temperature profile lines of the heaters, as shown in Figure S5c,d in the Supporting Information. Their relationship can be determined by these points, the current is approximately proportional to the voltage and the temperature is also about proportional to the square of voltage, which means that the resistance does not change even with increasing temperature by the heating.

The cyclic heating test of Ag FDs flexible heater (area, 3 cm × 3 cm) is investigated under the same DC voltage (2 V), as shown in Figure 4e. The saturation temperature run up to the same value and responses time are similar during ten heating cycles. Moreover, the highest temperature and lowest temperature are recovered quickly in heating cycles, which is very important for sensing,[59] thermochromics,[35] and thermotherapy[18] applications. In addition, Figure 4f presents the temperature response of the Ag FDs flexible heater for nine cycles in 9 d. There is a slight drop in saturation temperature at 2 V because of the surface of the heater, which is partially oxidized in ambient atmosphere.

Figure 5a shows thermal photographs of the Ag FDs flexible heater printed on different substrates. The saturation temperatures of the heaters printed on textile, PVA substrates are 60.3 and 65.3 °C, respectively, but the saturation temperature of the heaters printed on thermoplastic urethane (TPU) substrates is relative lower (≈45.2 °C) because of the poor printability caused higher resistivity of the TPU. As shown in Figure S6 in the Supporting Information, the sheet resistance of the printed heaters on different substrates sintered under room temperature and 60 °C, respectively. Figure 5b presents thermal photographs of the heaters with different patterns (quadrate mesh, hexagon mesh, and rhombus mesh), and their saturation temperatures are 64.8, 62.8, and 54.9 °C, respectively. The main reason is that actual heating area are different, the actual area of the quadrate mesh accounts for

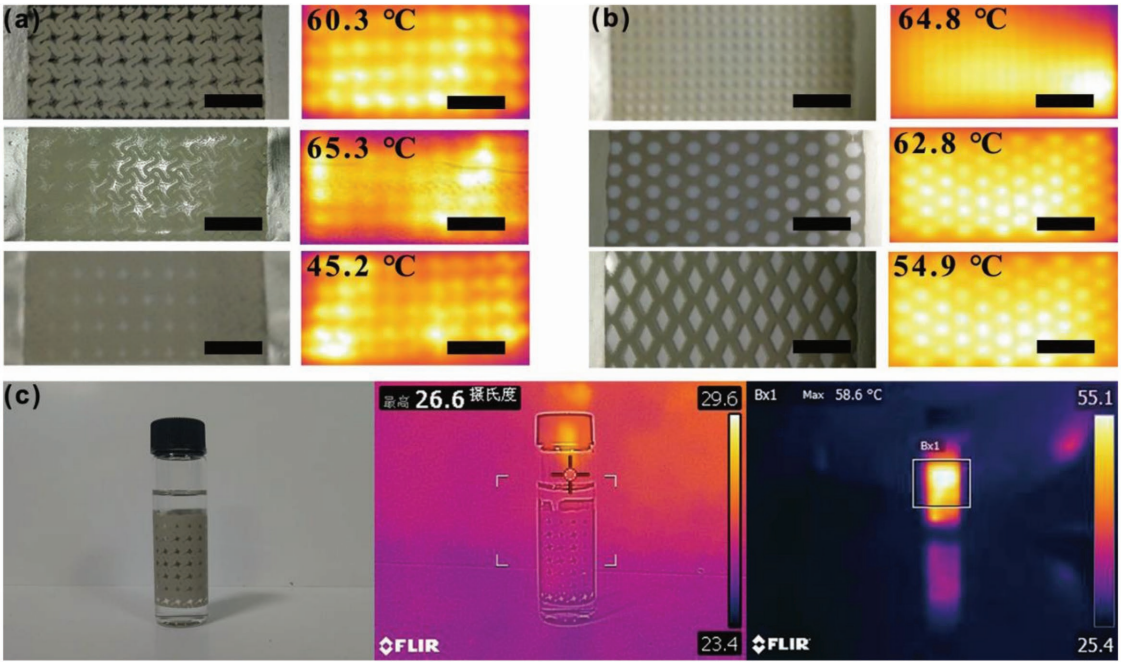

Figure 5. a) Thermal photographs of the Ag FDs flexible heater printed on different substrates (from top to bottom, textile, PVA, and TPU, scale bar is 1 cm). b) Thermal photographs for various heater designs (from top to bottom, quadrate mesh, hexagon mesh, and rhombus mesh, scale bar is 1 cm). c) (Left) Digital photograph of the Ag FDs flexible heater attached to the glass vial, and the thermal photographs under (middle) room temperature and (right) 3 V DC voltage, respectively.

≈56% (4.48 cm^2) of the total area (4 cm × 2 cm) (hexagon mesh, 4.24 cm^2 ≈53%, rhombus mesh, 3.92 cm^2 ≈49%). The results are in agreement with Figure 2b. Figure 5c (left) demonstrates that the flexible heater attached well with the glass vial because of the PET is lightweight and bendable. And the middle picture of Figure 5c shows that the thermal photographs of the Ag FDs flexible heater attached to the glass vial under room temperature. The saturation temperature of the heaters attached to glass vial up to 58.6 °C under 3 V DC, as shown in Figure 5c (right).

Screen printing technology can realize the low-cost and large area flexible electronics of preparation. Herein, a large scale flexible heater (12 cm × 5 cm) is fabricated via screen printing, as shown in **Figure 6**a. Figure 6b demonstrates that the flexible heater is well adapted to human wrist, because of excellent mechanize flexibility of the devices. Compared with previous study, the saturation temperature of the heater with 2.5 cm × 2.5 cm only reaches ≈40 °C under 5 V DC voltage,[35] but in this work, the saturation temperature of the Ag FDs flexible heater with a large area (12 cm × 5 cm) also can reach ≈39 °C under 5 V, as shown in Figure 6c. A portable energy provides the power of the heater, as shown in Figure S7 in the Supporting Information. Figure 6d shows the thermal photograph of the large area heater in release state. In addition, Figure 6e presents that the flexible heater is printed into a "2018" pattern on textile and attached well with cloth for heating or display. Figure 6f shows the saturation temperature of the heater attached to the cloth surface reaches 58 °C under

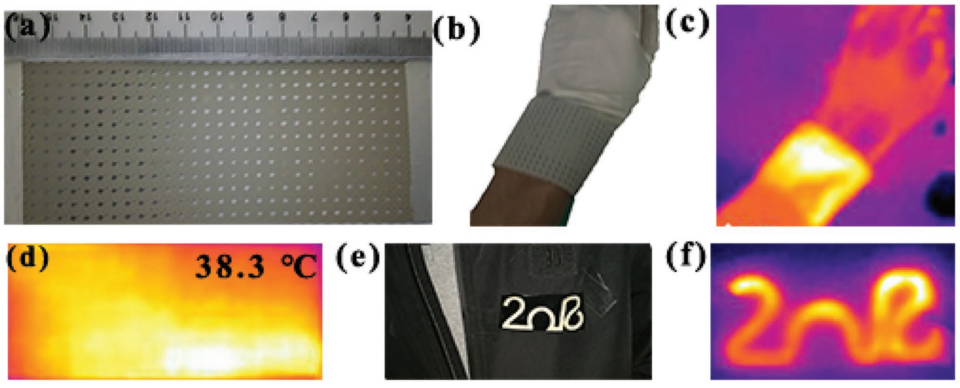

Figure 6. a) Digital photograph of the large-scale pattern flexible heater (area, 12 cm × 5 cm) printed on PET. b) Digital photograph and c) thermal photograph of the heater attached to human wrist. d) Thermal photograph of the heater in release state. e) Digital photograph and f) thermal photograph of the "2018" flexible heater printed on textile attached to the cloth.

≈5 V, indicating that the heaters can be driven by low voltage, which is feasible.

3. Conclusion

In summary, the Ag FDs with unique structures are synthesized via a facile redox process under ambient conditions. Then the as-obtained Ag FDs are hybrid with SIS solution to formulate conductive inks for manufacturing all-printed, versatile patterns and flexible heaters through screen-printing technology, which occupied with low-temperature sintering property (≈0.83 Ω sq^{-1} at 60 °C). The flexible heaters can be generally printed on the substrates of PET, TPU, PVA, and textile. Especially, the flexible heater printed on PET substrate exhibits high saturation temperature (≈135 °C), rapid response time (≈35 s), and low power consumption (≈209.67 °C cm^2 W^{-1}) at 4 V DC voltage, and negligible changes in saturation temperature after ten heating cycles. And importantly, the fabricated large scale flexible heaters are applied in the practical of wearable human wrist. We envision that the fully printed flexible heaters in this work exhibit enormous potential for flexible and wearable thermotherapy.

4. Experimental Section

Materials: Silver nitrate ($AgNO_3$, analytical reagent (AR)) and xylenes (C_8H_{10}, AR) were purchased from Sinopharm Chemical Reagent Co., Ltd. Hydroxylamine solution (NH_2OH, 50 wt% in water) and SIS (14 wt%) were purchased from Sigma-Aldrich Co., Ltd. Deionized water (18.2 MΩ) was used in this whole experiments.

Synthesis of Ag FDs: The Ag FDs were synthesized through the reduction of $AgNO_3$ by NH_2OH, which was operated at room temperature. Typically, 0.51 g of $AgNO_3$ and 715 µL of NH_2OH were dissolved in deionized water (50 mL), respectively. And the two solutions were uniformly mixed together by constant pressure funnel at the same rate of 3–5 mL min^{-1}. And the solutions were mixed in a three-necked round bottom flask, which were stirred vigorously on the magnetic stirrer. The products were washed for several times by using deionized water and anhydrous ethanol, respectively, then dried in a vacuum oven at 60 °C for further formulate of the Ag FDs-based inks.

Formulation of Ag FDs-Based Screen-Printable Inks: The inks were formulated by mixing Ag FDs with SIS. First, 3 g of SIS was dissolved in xylenes (24 mL), intensely stirred for 4 h at a speed of 800 rpm min^{-1}. 0.3 g of the Ag FDs particles and 700 µL of the SIS solution were evenly mixed together to formulate the inks.

Fabrication of the Ag FDs Flexible Heaters: The Ag FDs flexible heaters are fabricated by screen printing. Flexible heaters with versatile patterns are printed on different substrates (such as PET, PVA film, TPU film, and cloth) using a 300 mesh counts screen, followed by drying at 60 °C for 20 min to remove solvent. Then the electrodes on both sides of the Ag FDs flexible heaters are made with silver paste and dry at 60 °C for 40 min.

Characterizations: The morphologies of Ag FDs are characterized by SEM (Hitachi S-4800) and TEM (FEI Tecnai G20). The structure of Ag FDs is characterized by XRD (PANalytical X'Pert Pro with Cu *Kα* radiation). The sheet resistance of flexible heaters is measured by using four-probe resistance tester (FP-001). The heaters are fixed on a customized stage to study real-time sheet resistance under bend stress using a Keithley 2400 sourcemeter. The thermal properties of flexible heaters are performed by an IR camera (FLIR C3). The maximum temperatures of the flexible heaters are analyzed by the matching analysis tool (FLIR Tools+, FLIR System). The flexible heater experiments were performed in compliance with the relevant laws and approval of the Ethical Committee of Wuhan University Central South Hospital. Informed consent of the participant involved in the experiments has been obtained.

Supporting Information

Supporting Information is available from the Wiley Online Library or from the author.

Acknowledgements

P.Z. and B.T. contributed equally to this work. This work was supported by the National Natural Science Foundation of China (NSFC) (51471121), Hubei Provincial Natural Science Foundation (2014CFB261), Basic Research Plan Program of Shenzhen City (JCYJ20160517104459444), Natural Science Foundation of Jiangsu Province (BK20160383), and Wuhan University. All authors contributed during the preparation of the paper. All authors have given approval to the final version of the paper.

Conflict of Interest

The authors declare no conflict of interest.

Keywords

Ag fractal dendrites, flexible resistance heaters, printed electronics, screen printing, wearable electronics

Received: September 19, 2018
Revised: October 16, 2018
Published online: November 28, 2018

[1] W. Wu, *Nanoscale* **2017**, *9*, 7342.
[2] A. J. Bandodkar, I. Jeerapan, J. M. You, R. Nunez-Flores, J. Wang, *Nano Lett.* **2016**, *16*, 721.
[3] Z. Li, T. Le, Z. Wu, Y. Yao, L. Li, M. Tentzeris, K.-S. Moon, C. P. Wong, *Adv. Funct. Mater.* **2015**, *25*, 464.
[4] X. Huang, T. Leng, X. Zhang, J. C. Chen, K. H. Chang, A. K. Geim, K. S. Novoselov, Z. Hu, *Appl. Phys. Lett.* **2015**, *106*, 203105.
[5] A. G. Kelly, T. Hallam, C. Backes, A. Harvey, A. S. Esmaeily, I. Godwin, J. Coelho, V. Nicolosi, J. Lauth, A. Kulkarni, S. Kinge, L. D. A. Siebbeles, G. S. Duesberg, J. N. Coleman, *Science* **2017**, *356*, 69.
[6] K. Fukuda, T. Someya, *Adv. Mater.* **2017**, *29*, 1602736.
[7] X. Cao, C. Lau, Y. Liu, F. Wu, H. Gui, Q. Liu, Y. Ma, H. Wan, M. R. Amer, C. Zhou, *ACS Nano* **2016**, *10*, 9816.
[8] M. K. Choi, J. Yang, K. Kang, D. C. Kim, C. Choi, C. Park, S. J. Kim, S. I. Chae, T. H. Kim, J. H. Kim, T. Hyeon, D. H. Kim, *Nat. Commun.* **2015**, *6*, 7149.

[9] C. Jiang, Z. Zhong, B. Liu, Z. He, J. Zou, L. Wang, J. Wang, J. Peng, Y. Cao, *ACS Appl. Mater. Interfaces* **2016**, *8*, 26162.
[10] L. Huang, Y. Huang, J. Liang, X. Wan, Y. Chen, *Nano Res.* **2011**, *4*, 675.
[11] R. K. Mishra, L. J. Hubble, A. Martin, R. Kumar, A. Barfidokht, J. Kim, M. M. Musameh, I. L. Kyratzis, J. Wang, *ACS Sens.* **2017**, *2*, 553.
[12] Q. Lu, L. Liu, S. Yang, J. Liu, Q. Tian, W. Yao, Q. Xue, M. Li, W. Wu, *J. Power Sources* **2017**, *361*, 31.
[13] Y. Xu, M. G. Schwab, A. J. Strudwick, I. Hennig, X. Feng, Z. Wu, K. Müllen, *Adv. Energy Mater.* **2013**, *3*, 1035.
[14] J. Yeo, G. Kim, S. Hong, M. S. Kim, D. Kim, J. Lee, H. B. Lee, J. Kwon, Y. D. Suh, H. W. Kang, H. J. Sung, J.-H. Choi, W.-H. Hong, J. M. Ko, S.-H. Lee, S.-H. Choa, S. H. Ko, *J. Power Sources* **2014**, *246*, 562.
[15] A. Kamyshny, S. Magdassi, *Small* **2014**, *10*, 3515.
[16] T. R. Hebner, C. C. Wu, D. Marcy, M. H. Lu, J. C. Sturm, *Appl. Phys. Lett.* **1998**, *72*, 519.
[17] S. Choi, J. Park, W. Hyun, J. Kim, J. Kim, Y. B. Lee, C. Song, H. J. Hwang, J. H. Kim, T. Hyeon, D.-H. Kim, *ACS Nano* **2015**, *9*, 6626.
[18] W. Lan, Y. Chen, Z. Yang, W. Han, J. Zhou, Y. Zhang, J. Wang, G. Tang, Y. Wei, W. Dou, Q. Su, E. Xie, *ACS Appl. Mater. Interfaces* **2017**, *9*, 6644.
[19] R. F. Loeser, S. R. Goldring, C. R. Scanzello, M. B. Goldring, *Arthritis Rheum.* **2012**, *64*, 1697.
[20] A. J. Hartz, M. E. Fischer, G. Bril, S. Kelber, D. Rupley, jr, B. Oken, A. A. Rimm, *J. Chronic Dis.* **1986**, *39*, 311.
[21] L. Brosseau, K. A. Yonge, V. Welch, S. Marchand, M. Judd, G. A. Wells, P. Tugwell, *Cochrane Database of Systematic Reviews*, **2003**, *4*, CD004522.
[22] N. Kwon, K. Kim, J. Heo, I. Yi, I. Chung, *Nanotechnology* **2014**, *25*, 265702.
[23] T. Kim, Y. W. Kim, H. S. Lee, H. Kim, W. S. Yang, K. S. Suh, *Adv. Funct. Mater.* **2013**, *23*, 1250.
[24] D. Lordan, M. Burke, M. Manning, A. Martin, A. Amann, D. O'Connell, R. Murphy, C. Lyons, A. J. Quinn, *ACS Appl. Mater. Interfaces* **2017**, *9*, 4932.
[25] R. Gupta, K. D. Rao, K. Srivastava, A. Kumar, S. Kiruthika, G. U. Kulkarni, *ACS Appl. Mater. Interfaces* **2014**, *6*, 13688.
[26] M. Bobinger, J. Mock, P. La Torraca, M. Becherer, P. Lugli, L. Larcher, *Adv. Mater. Interfaces* **2017**, *4*, 1700568.
[27] B. Zhou, Y. Li, G. Zheng, K. Dai, C. Liu, Y. Ma, J. Zhang, N. Wang, C. Shen, Z. Guo, *J. Mater. Chem. C* **2018**, *6*, 8360.
[28] H.-J. Kim, Y. Kim, J.-H. Jeong, J.-H. Choi, J. Lee, D.-G. Choi, *J. Mater. Chem. A* **2015**, *3*, 16621.
[29] Y. Guo, G. Xu, X. Yang, K. Ruan, T. Ma, Q. Zhang, J. Gu, Y. Wu, H. Liu, Z. Guo, *J. Mater. Chem. C* **2018**, *6*, 3004.
[30] J. Liang, K. Tong, Q. Pei, *Adv. Mater.* **2016**, *28*, 5986.
[31] W. Dang, V. Vinciguerra, L. Lorenzelli, R. Dahiya, *Flexible Printed Electron.* **2017**, *2*, 013003.
[32] L. Liu, Q. Lu, S. Yang, J. Guo, Q. Tian, W. Yao, Z. Guo, V. A. L. Roy, W. Wu, *Adv. Mater. Technol.* **2018**, *3*, 1700206.
[33] K. Fukuda, Y. Takeda, Y. Yoshimura, R. Shiwaku, L. T. Tran, T. Sekine, M. Mizukami, D. Kumaki, S. Tokito, *Nat. Commun.* **2014**, *5*, 4147.
[34] Z. Ouyang, S. N. Lou, D. Lau, J. Chen, S. Lim, P.-C. Hsiao, D.-W. Wang, R. Amal, Y. H. Ng, A. Lennon, *Adv. Energy Mater.* **2017**, *7*, 1602325.
[35] C. Celle, C. Mayousse, E. Moreau, H. Basti, A. Carella, J.-P. Simonato, *Nano Res.* **2012**, *5*, 427.
[36] S. Hong, H. Lee, J. Lee, J. Kwon, S. Han, Y. D. Suh, H. Cho, J. Shin, J. Yeo, S. H. Ko, *Adv. Mater.* **2015**, *27*, 4744.
[37] Y. Kim, H. R. Lee, T. Saito, Y. Nishi, *Appl. Phys. Lett.* **2017**, *110*, 153301.
[38] T. J. Kang, T. Kim, S. M. Seo, Y. J. Park, Y. H. Kim, *Carbon* **2011**, *49*, 1087.
[39] Y. H. Yoon, J. W. Song, D. Kim, J. Kim, J. K. Park, S. K. Oh, C S. Han, *Adv. Mater.* **2007**, *19*, 4284.
[40] X. Sun, M. Zhao, B. Han, H. Kang, Z. Fan, Y. Liu, A. Umar, Z. Guo, *J. Nanosci. Nanotechnol.* **2018**, *18*, 3427.
[41] J. Kang, H. Kim, K. S. Kim, S. K. Lee, S. Bae, J. H. Ahn, Y. J. Kim, J. B. Choi, B. H. Hong, *Nano Lett.* **2011**, *11*, 5154.
[42] C. Wang, V. Murugadoss, J. Kong, Z. He, X. Mai, Q. Shao, Y. Chen, L. Guo, C. Liu, S. Angaiah, Z. Guo, *Carbon* **2018**, *140*, 696.
[43] Z. Wang, R. Wei, J. Gu, H. Liu, C. Liu, C. Luo, J. Kong, Q. Shao, N. Wang, Z. Guo, X. Liu, *Carbon* **2018**, *139*, 1126.
[44] M. N. Gueye, A. Carella, R. Demadrille, J. P. Simonato, *ACS Appl. Mater. Interfaces* **2017**, *9*, 27250.
[45] Y. Li, J. Zhu, S. Wei, J. Ryu, L. Sun, Z. Guo, *Macromol. Chem. Phys.* **2011**, *212*, 1951.
[46] H.-S. Jang, S. K. Jeon, S. H. Nahm, *Carbon* **2011**, *49*, 111.
[47] S. Ji, W. He, K. Wang, Y. Ran, C. Ye, *Small* **2014**, *10*, 4951.
[48] A. Y. Kim, M. K. Kim, C. Hudaya, J. H. Park, D. Byun, J. C. Lim, J. K. Lee, *Nanoscale* **2016**, *8*, 3307.
[49] X. Zhang, X. Yan, J. Chen, J. Zhao, *Carbon* **2014**, *69*, 437.
[50] N. Wu, C. Liu, D. Xu, J. Liu, W. Liu, Q. Shao, Z. Guo, *ACS Sustainable Chem. Eng.* **2018**, *6*, 12471.
[51] Z. Yang, X. Hao, S. Chen, Z. Ma, W. Wang, C. Wang, L. Yue, H. Sun, Q. Shao, V. Murugadoss, Z. Guo, *J. Colloid Interface Sci.* **2019**, *533*, 13.
[52] R. Sivasubramanian, M. V. Sangaranarayanan, *Sens. Actuators, B* **2015**, *213*, 92.
[53] S. Sorel, D. Bellet, J. N. Coleman, *ACS Nano* **2014**, *8*, 4805.
[54] C. Hudaya, B. J. Jeon, J. K. Lee, *ACS Appl. Mater. Interfaces* **2015**, *7*, 57.
[55] F. Wu, P. Li, K. Sun, Y. Zhou, W. Chen, J. Fu, M. Li, S. Lu, D. Wei, X. Tang, Z. Zang, L. Sun, X. Liu, J. Ouyang, *Adv. Electron. Mater.* **2017**, *3*, 1700047.
[56] S. Zhao, Y. Gao, J. Li, G. Zhang, R. Sun, C.-P. Wong, *Carbon* **2015**, *95*, 987.
[57] S. Zhang, Y. Li, Q. Tian, L. Liu, W. Yao, C. Chi, P. Zeng, N. Zhang, W. Wu, *J. Mater. Chem. C* **2018**, *6*, 3999.
[58] S. Yao, J. Cui, Z. Cui, Y. Zhu, *Nanoscale* **2017**, *9*, 3797.
[59] N. Ishii, T. Kato, J. Abe, *Sci. Rep.* **2012**, *2*, 819.